HOKKAIDO UNIVERSITY

Title	Degenerative and regenerative features of myofibers differ among skeletal muscles in a murine model of muscular dystrophy
Author(s)	Ikeda, Teppei; Ichii, Osamu; Otsuka-Kanazawa, Saori; Nakamura, Teppei; Elewa, Yaser Hosny Ali; Kon, Yasuhiro
Citation	Journal of Muscle Research and Cell Motility, 37(4-5), 153-164 https://doi.org/10.1007/s10974-016-9452-6
Issue Date	2016-10
Doc URL	http://hdl.handle.net/2115/67282
Rights	The final publication is available at link.springer.com
Type	article (author version)
File Information	J Muscle Res Cell Motil v.37(4-5) p.153-164.pdf

Instructions for use

1 **Degenerative and regenerative features of myofibers differ among skeletal muscles in a murine**

2 **model of muscular dystrophy**

3

4 Teppei Ikeda, Osamu Ichii, Saori Otsuka-Kanazawa, Teppei Nakamura, Yaser Hosny Ali Elewa, Yasuhiro

5 Kon*

6

7 Laboratory of Anatomy, Department of Biomedical Sciences, Graduate School of Veterinary Medicine,

8 Hokkaido University, Sapporo 060-0818, Japan

9

10 ***Corresponding author:** Yasuhiro Kon, DVM, PhD,

11 Laboratory of Anatomy, Department of Biomedical Sciences, Graduate School of Veterinary Medicine,

12 Hokkaido University, Kita 18, Nishi 9, Kita-ku, Sapporo 060-0818, Japan.

13 Email: y-kon@vetmed.hokudai.ac.jp.

14 Tel: +81-11-706-5187

15 Fax: +81-11-706-5189

16

19

20   **Abstract**

21   Skeletal muscle myofibers constantly undergo degeneration and regeneration. Histopathological features

22   of 6 skeletal muscles (cranial tibial [CT], gastrocnemius, quadriceps femoris, triceps brachii [TB], lumbar

23   longissimus   muscles,   and   costal   part   of   the   diaphragm   [CPD])   were   compared   using

24   C57BL/10ScSn-Dmd^{mdx} (mdx) mice, a model for muscular dystrophy versus control, C57BL/10 mice.

25   Body weight and skeletal muscle mass were lower in mdx mice than the control at 4 weeks of age; these

26   results were similar at 6–30 weeks. Additionally, muscular lesions were observed in all examined skeletal

27   muscles in mdx mice after 4 weeks, but none were noted in the controls. Immunohistochemical staining

28   revealed   numerous   paired   box   7-positive   satellite   cells   surrounding   the   embryonic   myosin   heavy

29   chain-positive regenerating myofibers, while the number of the former and staining intensity of the latter

30   decreased as myofiber regeneration progressed. Persistent muscular lesions were observed in skeletal

31   muscles of mdx mice between 4–14 weeks of age, and normal myofibers decreased with age. Number of

32   muscular lesions was lowest in CPD at all ages examined, while the ratio of normal myofibers was lowest

33   in TB at 6 weeks. In CT, TB, and CPD, Iba1-positive macrophages, the main inflammatory cells in

34   skeletal muscle lesions, showed a significant positive correlation with the appearance of regenerating

35   myofibers.   Additionally,   B220-positive   B-cells   showed   positive   and   negative   correlation   with

36   regenerating and regenerated myofibers, respectively. Our data suggest that degenerative and regenerative

37   features of myofibers differ among skeletal muscles and that inflammatory cells are strongly associated

38   with regenerative features of myofibers in mdx mice.

39

40   **Key words**: muscular dystrophy, mdx mouse, skeletal muscle remodeling, inflammation, triceps brachii,

41   costal part of the diaphragm

42

43 **Abbreviations:** CT, cranial tibial muscle; CPD, costal part of the diaphragm; GA, gastrocnemius muscle;

44 HE, hematoxylin-eosin; LL, lumbar longissimus muscle; MRF, myogenic regulatory factor; MT,

45 Masson's trichrome stain; QR, quadriceps femoris muscle; TB, triceps brachii muscle

INTRODUCTION

47   Skeletal muscles have high regenerative ability and satellite cells, also known as myogenic precursor

48   cells, play a key role in muscle regeneration (Chargé and Rudnicki 2004). Skeletal muscle remodeling,

49   which involves degeneration and regeneration of myofibers, is a constant process in all animals. Aging,

50   metabolic diseases, hereditary muscle diseases and neuromuscular diseases can affect the processes

51   involved in skeletal muscle remodeling, which lead to breakdown and atrophy of skeletal muscle. Muscle

52   repair is a multistep process that includes myofiber degeneration and regeneration (Le Grand and

53   Rudnicki 2007; Ten Broek et al. 2010; Tsivitse 2010). Following damage to myofibers, satellite cells are

54   activated and proliferate to give rise to a population of transient, amplifying myogenic cells called

55   myoblasts, which express myogenic regulatory factors (MRFs) such as myogenic differentiation 1 and

56   myogenic factor 5. Myoblasts subsequently express another MRF called myogenin, commit to terminal

57   differentiation, and fuse to reconstruct their host myofibers or to generate new myofibers and repair

58   damaged tissue (Tedesco et al. 2010).

59   Duchenne muscular dystrophy (DMD), the most common and severe type of muscular dystrophy in

60   humans, is an X-linked, recessive, lethal muscle wasting disease affecting approximately 1 in 3,500 boys

61   (Emery 1989). It is caused by mutations in the *DMD* gene, located on the X chromosome, which codes

62   for dystrophin, a membrane-associated structural protein. Homologues of *DMD* have been identified in

63   several animals including dogs (Cooper et al. 1988), cats (Carpenter et al. 1989) and mice (Bulfield et al.

64   1984; Pastoret and Sebille 1995). C57BL/10ScSn-*Dmd*[mdx] (mdx) mice do not produce dystrophin, due to

65   a point-mutation in *Dmd*. Though these mice do not represent a complete phenotypic model of DMD in

66   humans, they have been used as a representative animal model of DMD (Bulfield et al. 1984). These mice

67   show pathological changes in skeletal muscles, characterized by necrosis of skeletal muscle fibers

68   accompanied by regeneration (Bulfield et al. 1984; Pastoret and Sebille 1995; Boland et al. 1995).

69   It has been observed that the pathological features of DMD differ among different types of skeletal

70   muscles. Skeletal muscles of the thoracic esophagus show no necrosis and no regenerating fibers in mdx

71 mice (Boland et al. 1995). However, large numbers of necrotic myofibers have been seen between 3 and 4

72 weeks of age in limb muscle (Shavlakadze et al. 2004), followed by regeneration of myofibers by 6 to

73 12 weeks of age (McGeachie et al. 1993). In contrast to the limb, muscles of the diaphragm show

74 progressive degeneration of myofibers (Stedman et al. 1991). Therefore, a comparison of

75 histopathological changes among the muscles of mdx mice would be useful to better understand the

76 pathological characteristics of DMD (Louboutin et al. 1993; Pastoret and Sebille 1995; Boland et al.

77 1995).

78   Inflammation is a crucial process that is thought to both, exacerbate damage and necrosis as well as

79 promote regeneration in skeletal muscles. Inflammatory cells, especially neutrophils and macrophages,

80 mediate necrosis of muscle cells via oxidative damage both, *in vitro* (Pizza et al. 2001; McLoughlin et al.

81 2003; Nguyen and Tidball 2003) and *in vivo* (Pizza et al. 2005; Cheung and Tidball 2003; Nguyen and

82 Tidball 2003), with macrophages also performing their principal role of phagocytizing necrotic cells

83 (Almekinders and Gilbert 1986; Robertson et al. 1993; Lescaudron et al. 1999; Merly et al. 1999;

84 Mojumdar et al, 2014). Further, it has been proposed that an excessive inflammatory response can directly

85 damage myofibers under myopathic conditions such as dystrophies or myositis (Porter et al. 2002).

86 Importantly, DNA microarray studies of mdx muscle show that 30% of all differentially expressed genes

87 are associated with inflammation (Porter et al. 2002; Porter et al. 2004; Tidball 2005).

88   In this study, we demonstrated that degenerative and regenerative features of myofibers differ among

89 skeletal muscles in mdx mice, and that these differences are associated with immune cell infiltration into

90 the skeletal muscle lesions. Each skeletal muscle in the adult mammalian body has a different character

91 based on anatomical, physiological, and/or mechanical factors such as exercise load and posture of the

92 animal. The findings of this study shed light on the process of muscle remodeling and the pathological

93 differences among different types of skeletal muscles in DMD.

94   **MATERIALS AND METHODS**

95   *Experimental animals*

96   Animal experimentation was approved by the Institutional Animal Care and Use Committee of the

97   Graduate School of Veterinary Medicine, Hokkaido University (approval No. 13-0032). Male, mdx mice

98   were purchased from Central Institute for Experimental Animals (Kanagawa, Japan) and control, male

99   C57BL/10SnSlc (B10) mice were purchased from Japan SLC (Shizuoka, Japan). Mice were housed in the

100   animal facility of Graduate School of Veterinary Medicine, Hokkaido University. The body weight of B10

101   and mdx mice was measured at 1 (B10, mdx; n = 4, 19, respectively), 2 (n = 4, 17), 3 (n = 4, 17), 4 (n =

102   10, 17), 6 (n = 5, 12), 8 (n = 5, 11), 14 (n = 5, 10), and 30 (n = 4, 4) weeks of age. Skeletal muscles were

103   harvested at 4 (n = 4), 6 (n = 4), and 14 (n = 4) weeks of age. The genotype of mdx mice was analyzed by

104   TaqMan PCR (Applied Biosystems, Foster, CA, USA) targeting a point mutation in the *DMD* gene.

105   Experimental animals were handled in accordance with the Guide for the Care and Use of Laboratory

106   Animals, Graduate School of Veterinary Medicine, Hokkaido University (approved by the Association for

107   Assessment and Accreditation of Laboratory Animal Care International).

108

109   *Tissue preparation and microscopic observation*

110   The caudal vena cava was cut under deep anesthesia by an intraperitoneal injection (0.012–0.015

111   ml/g of body weight) of 2.5% Avertin, while 4% paraformaldehyde was perfused from the left ventricle.

112   Six skeletal muscles (cranial tibial muscle, CT; gastrocnemius muscle, GA; quadriceps femoris muscle,

113   QR; triceps brachii muscle, TB; lumbar longissimus muscle, LL; and costal part of the diaphragm, CPD)

114   were collected. The muscles from the left side of the body were fixed in 10% neutral buffer formalin for

115   32–48 hours for morphological examination, while those from the right side of the body were fixed in 4%

116   paraformaldehyde for 18–24 hours for immunohistochemical staining. After fixation, specimens were

117   dehydrated in graded alcohol and embedded in paraffin. Subsequently, 2-µm-thick paraffin sections of

118   each skeletal muscle were deparaffinized, rehydrated, stained with hematoxylin-eosin (HE) and Masson's

119   trichrome stain (MT), and observed under a light microscope.

120

121   *Immunohistochemistry*

122   Immunohistochemical staining for embryonic myosin heavy chain (eMyHC), paired box 7 (PAX7),

123   Gr1 (Ly-6G), Iba1, B220, and CD3 was performed using 3-µm-thick paraffin sections to detect

124   regenerating myofibers, satellite cells, granulocytes, pan-macrophages (including M1/M2 macrophages;

125   Pierezan et al, 2014), B-cells, and pan T-cells, respectively. The paraffin sections were deparaffinized and

126   antigen was retrieved. After cooling, slides were soaked in methanol containing 3% H_2O_2 for 20 minutes

127   at room temperature to remove internal peroxidase. After washing, sections were blocked with mouse

128   blocking reagent (Nichirei, Tokyo, Japan) for eMyHC and PAX7, and with 10% normal goat serum

129   (Nichirei, Tokyo. Japan) for Gr1, Iba1, B220, and CD3, for 60 minutes at room temperature and incubated

130   with primary antibodies overnight, at 4°C. After washing thrice with phosphate-buffered saline, sections

131   were incubated with secondary antibodies for 30 minutes at room temperature, washed, and incubated

132   with streptavidin-biotin complex (SABPO® kit; Nichirei, Tokyo, Japan) for 30 minutes. The sections

133   were then incubated with 3,3′-diaminobenzidine tetrahydrochloride-H_2O_2 solution. Finally, the sections

134   were lightly counterstained with hematoxylin. Details of the antigen retrieval method as well as the

135   source and dilution of the antibodies are listed in Table 1.

136

137   *Histoplanimetry*

138   Quantitative analysis of degenerative and regenerative myofibers was performed using ImageJ

139   (http://rsb.info.nih.gov/ij/) software, as previously described (Pastoret and Sebille 1995). Briefly, opaque

140   as well as faintly colored fibers, frequently filled with phagocytes were classified as degenerating

141   myofibers. Small fibers in which, the cytoplasm takes on a uniformly bluish color, with central vesicular

142   nuclei were classified as regenerating myofibers. Fibers with non-peripheral nuclei and eosinophilic

143   cytoplasm were classified as regenerated myofibers. All others were classified as normal myofibers. All

7

144   myofibers in transverse sections of each skeletal muscle were counted (at least 2,000 myofibers per

145   specimen) and classified into 1 of the 4 types of myofibers described above. Based on

146   immunohistochemical staining, the number of Gr1-, Iba1-, B220-, and CD3-positive cells in each skeletal

147   muscle was counted, and the total area of transverse sections of each skeletal muscle was then measured.

148   Finally, the number of immune-positive cells was divided by the total area of transverse sections of each

149   skeletal muscle, and these values were expressed as cell number per unit area (number/mm^2).

150

151   *Statistical analysis*

152   All numerical results are presented as mean ± standard error (SE) and analyzed using non-parametric

153   methods. The Mann-Whitney *U*-test was used to compare 2 groups ($P < 0.05$). The Kruskal-Wallis test

154   was used to compare 3 or more groups, and multiple comparisons were performed using Scheffé's

155   method when a significant difference was observed ($P < 0.05$). Correlation between myofibers exhibiting

156   histopathological changes and immune cell numbers in the skeletal muscle lesions was analyzed by

157   Spearman's correlation coefficient test (ρ) ($P < 0.05$).

158   **Results**

159   *Body weight and skeletal muscle mass in mdx and B10 mice*

160   Changes in body weight and skeletal muscle mass were compared between mdx and B10 mice from

161   1 to 30 weeks of age. Body weight was similar between the 2 groups up to 3 weeks of age. However, at

162   4 weeks, the body weight of mdx mice was significantly lower than that of B10 mice (Figure 1A). From 6

163   weeks onwards, body weight was similar again between the two groups. Gross anatomical and

164   histological examination at 4 weeks of age revealed that the muscle mass of mdx mice was markedly

165   lower compared to that of B10 mice. Accordingly, the skeletal muscle area in the transverse sections of all

166   examined skeletal muscles was reduced in mdx mice than in B10 mice at 4 weeks of age (Figure 1B).

167   Muscular histopathological changes, such as degenerative and atrophied myofibers, were widely but

168   focally observed in mdx mice, but not in B10 mice (Figure 1B). However, at 6 weeks of age, the skeletal

169   muscle areas of mdx mice seemed to increase to almost equal levels to those in B10 mice (Figure 1C). In

170   mdx mice, myofibers with non-peripheral nuclei occupied the observed area at 6 weeks (Figure 1C). In

171   addition to the results of body weight change and muscle features (Figure 1), we considered previous

172   reports (Shavlakadze et al. 2004; McGeachie et al. 1993) and examined ages and divided the mdx mouse

173   group into the muscle degenerative phase (4 weeks of ages), muscle regenerative phase (6 weeks onward),

174   and the sexually matured and muscle regenerated phase (14 weeks).

175

176   *Histopathological features of skeletal muscle in mdx and B10 mice*

177   We analyzed the histopathological changes shown in Figure 1B in more detail. As shown in Figure 2,

178   B10 mice showed no histological changes in any of the examined muscles. In mdx mice, on the other

179   hand showed no histopathological changes in skeletal muscles at 2 weeks of age, and very few changes at

180   3 weeks (data not shown). However, severe histopathological changes were observed from 4 weeks of age

181   (Figure 2). Muscular lesions were observed focally in all mdx mice at all examined ages. These lesions

182   consisted of 3 types of myofibers: degenerative myofibers (arrows in Figure 2), regenerating myofibers

9

183   (small arrowheads in Figure 2), and regenerated myofibers (large arrowheads in Figure 2). Although these

184   muscular lesions were observed in all examined muscles of mdx mice, the number of degenerative

185   myofibers tended to be lower in CPD compared to other skeletal muscles (Figure 2). These results suggest

186   that the progression of histopathological changes in mdx mice may differ among skeletal muscles.

187   To further investigate regenerative features of myofibers in mdx mice, immunohistochemical

188   staining was carried out. Numerous PAX7-positive muscle satellite cells surrounded eMyHC-positive

189   regenerating myofibers in skeletal muscles of mdx mice (Figure 3A–F), and the number of the former and

190   the staining intensity of the latter gradually decreased with the progression of myofiber regeneration

191   (Figure 3A–C and G–L).

192

193   *Histopathological changes in different skeletal muscles of mdx mice*

194   To compare the muscular lesions among examined skeletal muscles in mdx mice, we compared the

195   ratio   of   the   number   of   fibers   classified   as   normal,   degenerative,   and   centronucleated

196   (regenerating/regenerated) to the total number of muscle fibers in each skeletal muscle examined

197   (Figure 4). Although all examined skeletal muscles contained muscular lesions during the observation

198   period, the ratio of each type of myofiber differed among skeletal muscles. The ratios of normal and

199   degenerative myofibers were larger and smaller, respectively, in CPD compared with other muscles at 4

200   weeks of age (Figure 4A and B). The ratios of normal myofibers also tended to be larger in CPD than in

201   the other muscles at 6 and 14 weeks of age (Figure 4A). Further, the ratio of centronucleated myofibers,

202   indicating regenerating or regenerated myofibers, tended to be smaller in CPD than in the other muscles

203   (Figure 4C). Significant differences between CPD and the other muscles were observed in terms of ratio

204   of regenerated myofibers and that of regenerating myofibers (Figure 4D and E). At 6 weeks of age, the

205   ratio of normal myofibers was significantly smaller in TB as compared to that in CT, GA, and CPD. In

206   addition to these variations among different skeletal muscles, significant differences were noted in

207   muscular lesions with respect to ratios, within the same skeletal muscle. The ratio of normal and

208   centronucleated myofibers, especially regenerated myofibers, were smaller and larger, respectively, at 14

209   as compared to 4 weeks of age, in all examined muscles (Figure 4A, C, and E). These results indicate that

210   the pathological features of muscular lesions differed among skeletal muscles and with age. In particular,

211   CPD and TB tended to show milder and severer lesions, respectively, compared with other examined

212   skeletal muscles, in mdx mice.

213

214   *Distribution of immune cells in skeletal muscle lesions*

215   Since morphological analysis using HE and/or MT staining indicated the presence of macrophages

216   and granulocytes (especially neutrophils) in the muscular lesions (Figure 2 and 3D), the distribution of

217   immune cells was analyzed by immunohistochemistry. Histopathological analyses described above

218   indicated that TB and CPD showed different features of muscular lesions compared with the other

219   skeletal muscles examined. Therefore, immunohistochemical analysis was performed for TB, CPD, and

220   CT muscles, where CT served as control. Immunohistochemical staining revealed the presence of Iba1-,

221   Gr1-, B220-, and CD3-positive cells in the skeletal muscle lesions of mdx mice (Figure 5A–D). All

222   positive reactions were counted and normalized by the area of each skeletal muscle. Iba1- and

223   Gr1-positive cells were high in TB at 4 weeks of age and low in TB and CPD at 14 weeks of age, but no

224   significant differences were noted in any skeletal muscle with respect to age (Figure 5E and F).

225   B220-positive cells in CT and TB, whereas CD3-positive cells in TB were significantly higher at 4 weeks

226   of age as compared to those at 6 and 14 weeks of age (Figure 5G and H). A significant difference in the

227   number of immune cells in the examined skeletal muscles at the same age was observed only in CD3 at

228   14 weeks of age. CPD showed a large number of CD3-positive cells compared to CT, at 14 weeks of age

229   (Figure 5H). The number of Iba1-positive cells was the highest of the 4 immune cells examined, in all

230   skeletal muscles at the same age (Figure 5E).

231

232   *Correlation between histopathological changes in skeletal muscles and immune cell numbers*

233   As shown in Figure 6, a significant correlation was observed between Iba1-positive cells and

234   regenerating myofibers (Figure 6B), between Gr1 and regenerated myofibers (Figure 6F), and between

235   B220-positive cells and regenerated myofibers (Figure 6I).

236

237 **Discussion**

238   The present study demonstrated that degenerative and regenerative features of myofibers differ

239 among skeletal muscles in mdx DMD model mice. Body weight of mdx mice was significantly lower

240 than that of B10 mice at 4 weeks of age, but was similar at 6 weeks. Myofiber necrosis has been

241 previously observed in mdx mice at 3 weeks of age, followed by myofiber regeneration (Coulton et al.

242 1988; McGeachie et al. 1993; Grounds and Torrisi 2004). Additionally, a large number of necrotic

243 myofibers have been observed between 3 and 4 weeks of age in CT muscle (Shavlakadze et al. 2004).

244 After onset of acute myofiber necrosis, degeneration of skeletal muscle decreases accompanied by

245 regeneration of myofibers and is at a low level by 6 to 12 weeks of age (McGeachie et al. 1993). In the

246 present study, the skeletal muscle area was smaller in mdx mice than in B10 mice in transverse sections

247 of all examined skeletal muscles at 4 weeks of age, but was comparable at 6 weeks. This recovery of

248 the skeletal muscle area is thought to be the result of acute regeneration of myofibers. Further, Pastoret

249 and Sebille (1995) compared the body weight and CT muscles of mdx and B10 mice from 2 to 104

250 weeks of age, resulting that mdx mice showed higher body weight than B10 mice from 13 to 26 weeks

251 of age, due to hypertrophy of mdx skeletal muscle. Therefore, hypertrophy of skeletal muscle could be

252 one of the morphological features of myofiber regeneration in mdx mice. A significant difference in

253 body weight of mdx and B10 mice at 4 weeks of age was observed in the present study, which may be

254 due to degeneration of skeletal muscles in mdx mice.

255   From 4 weeks of age onwards, skeletal muscle lesions containing degenerating, regenerating, or

256 regenerated myofibers were observed in mdx mice. Different muscles have been analyzed in mdx mice

257 after exercise (Weller et al. 1990; Brussee et al. 1997; Granchelli et al. 2000; De Luca et al. 2005),

258 administration of drugs (Hodgetts et al. 2006), engraftment of somatic cells (Hindi et al. 2013; Boldrin

259 et al. 2015), and gene modification (Li et al. 2009; Heydemann et al. 2012). The results obtained and

260 the skeletal muscles analyzed are different in these previous reports. The present study compared 6

261 skeletal muscles: CT, GA, QR, TB, LL, and CPD at 4, 6 and 14 weeks of age and found that the extent

13

262   of degeneration and regeneration differs among skeletal muscles with age, in mdx mice. CPD tended to

263   show less pathological changes than other skeletal muscles in mdx mice during the examined period. A

264   similar observation was reported by Louboutin et al., who demonstrated that histopathological changes

265   in the mdx diaphragm are rare before 25 days of age, whereas the degeneration of myofibers begins at

266   21-25 days of age in the hind limb muscles (extensor digitorum longus: EDL, CT, and soleus).

267   Additionally, regenerating fibers with central nuclei were fewer in the diaphragm than in hind limb

268   muscles during the observation period of 30 to 270 days of age (Louboutin et al. 1993). Boland et al.

269   also showed a lower number of myofibers with central nuclei and a higher number of myofibers with

270   peripheral nuclei in the diaphragm than in CT and rectus abdominis muscles of mdx mice during 12-18

271   months of age (Boland et al., 1995). Although the pathological implications of nuclear position in

272   muscle diseases might be debatable, these data and a recent study showed skeletal muscle fibers with

273   central nuclei as regenerated myofibers (Boldrin et al., 2015); thus we considered that central nuclei

274   could be used as a marker of regeneration. In the present study, CPD tended to show a higher ratio of

275   normal fiber as compared to the other skeletal muscles, especially at 4 weeks of age. Regeneration of

276   myofibers begins after degeneration and the number of regeneration fibers increased clearly with age in

277   CPD of mdx mice. This indicates that CPD shows late-onset degeneration of myofibers. However,

278   Louboutin *et al*. also showed that fibrosis, occasionally including adipose tissue replacement, is

279   observed at 270 days of age in the diaphragm, but was less-frequent in hind limb muscles (Louboutin et

280   al. 1993), indicating that CPD might have lower regenerative ability as compared to other skeletal

281   muscles. Fiber-type transition is a pathological response against contraction-induced injury in DMD

282   (Gehrig et al. 2010). However, Schneider et al. observed the diaphragm as a severely affected

283   muscle in DMD and examined the fiber-type switch compared with quadriceps (a fast-twitch

284   muscle) and soleus (a slow-twitch muscle) in 2-month-old mouse models of DMD. They reported

285   fiber-type transition from fast-fiber (type 2b) to slow-fiber (type 1 and type 2a) in all of the 3

286   muscles; however, type 1 MyHC and eMyHC are not co-expressed, suggesting that regeneration

287   and fiber-type switch are two independent mechanisms in the dystrophic muscles (Schneider et al.,

288   2013).

289   In addition, the present study shows that increased muscular lesions are observed in TB compared

290   to the other skeletal muscles at 6 weeks of age. Brussee *et al.* also reported that TB of mdx mice

291   showed more atrophied myofibers than CT, EDL, soleus, GA, biceps brachii, and diaphragm muscles

292   under sedentary conditions (Brussee et al. 1997). Interestingly, they also showed that the severity of

293   muscle damage among skeletal muscles differed after 3 days of downhill running exercise compared to

294   sedentary conditions (Brussee et al. 1997). The present study shows that the degree of degeneration and

295   regeneration, involving damage to myofibers or subsequent reactions of muscular satellite cells or

296   myoblasts, differs among skeletal muscles, which may have an effect on the phenotypes of mdx mice.

297   The difference in muscle pathological features in mdx mice has been examined in several previous

298   reports (Louboutin et al. 1993; Brussee et al. 1997); however, their inflammatory features in different

299   muscles are scarcely addressed. The present study demonstrated that Iba1-positive macrophages are the

300   major inflammatory cells in skeletal muscle lesions that positively correlate with the number of

301   regenerating myofibers, whereas Gr1-positive granulocytes, mainly neutrophils, negatively correlate

302   with regenerated myofibers in mdx mice. After muscle injury caused by trauma such as extensive

303   physical activity, or by innate genetic defects, inflammatory cells such as neutrophils and macrophages

304   infiltrate into the lesions (Belcastro et al. 1996). Necrosis of myofibers is the initial event in skeletal

305   muscle degeneration, accompanied by the activation of mononucleated cells, principally inflammatory

306   and myogenic cells. Neutrophils are the first inflammatory cells to infiltrate the injured muscle, with a

307   significant increase in their numbers as early as 1–6 h after myotoxin- or exercise-induced muscle

308   damage (Orimo et al. 1991; Fielding et al. 1993). Some reports revealed that prevention of neutrophil

309   infiltration after injury reduces force deficits and histological damage to muscle fibers (Walden et al.

310   1990; Brickson et al. 2003; Pizza et al. 2005; Lockhart and Brooks 2008), suggesting that neutrophils

311   contribute to muscle fiber damage. In the present study, although neutrophils did not show a correlation

312 with degenerating myofibers, a negative correlation with regenerated myofibers was noted, indicating

313 that neutrophils decrease with progression of regeneration. After neutrophil infiltration, macrophages

314 become the predominant inflammatory cell type within the site of injury (Orimo et al. 1991; Tidball

315 2005). Macrophages, especially the M2-type, infiltrate the injured site to phagocytose cellular debris

316 and may affect other aspects of muscle regeneration by activating myogenic cells (Almekinders and

317 Gilbert 1986; Robertson et al. 1993; Lescaudron et al. 1999; Merly et al. 1999). Muscle degeneration is

318 followed by the activation of a muscle repair process. Myogenic cells differentiate and fuse to existing

319 damaged fibers for repair or to one another for new myofiber formation (Snow 1977; Snow 1978; Darr

320 and Schultz 1987). Muscle regeneration is slower in older animals, which coincides with weakened

321 phagocytosis activity by inflammatory cells (Zacks and Sheff MF 1982; Grounds 1987). In addition,

322 mouse strains with slower rates of phagocytic removal of muscle debris show slower rates of muscle

323 regeneration (Grounds 1987). No significant difference in Iba1- and Gr1-positive cell infiltration was

324 observed among muscles in the present study; however, many studies support the hypothesis that

325 phagocytosis is a necessary feature of muscle repair, and that macrophages and neutrophils play an

326 important role in this process.

327   The present study also revealed that B220-positive, B cells were negatively correlated with

328 regenerated myofibers. Several studies suggest that B- and T-cells contribute to the development of

329 muscle fibrosis in aged (> 12 months) SCID-mdx (Farini et al. 2007) and nu/nu-mdx mice (Morrison et

330 al. 2000). The absence of B and T cells results in reduced fibrosis, accompanied by a reduction of

331 transforming growth factor-β1 (Farini et al. 2007). In the present study, although the number of B

332 and/or T cells was significantly lower than that of macrophages (data not shown) and slightly lower

333 than that of neutrophils, in all examined skeletal muscles at each age, numbers of both B and T cells

334 were significantly higher in TB at 4 weeks of age compared to that at 6 and 14 weeks of age, suggesting

335 their importance in the early stages of muscular dystrophy in mdx mice.

336   In conclusion, the degenerative and regenerative features of myofibers in mdx mice differ among

337   skeletal muscles. Inflammatory cells, especially phagocytes and B cells, are strongly associated with

338   the regenerative features of myofibers. Though the triggers for these pathological differences are

339   unknown, anatomical, physiological, and/or mechanical factors such as exercise load may affect these

340   differences in remodeling processes among examined skeletal muscles. Further research involving the

341   study of muscle cells using cell-specific markers and quantification of MRFs in skeletal muscles, is

342   required to further understand muscular remodeling.

343

344   **Authors' contributions**

345   YK conceptualized the study. TI, OI, TN, YE, and YK designed the experiments. TI performed the

346   experiments and analyzed the data. TI, OI, and YK drafted the manuscript.

347

348   **Disclosures**

349   The authors declare no conflicts of interest.

350

351 **References**

352 Almekinders LC, Gilbert JA (1986) Healing of experimental muscle strains and the effects of nonsteroidal

353 anti-inflammatory medication. Am J Sports Med 14:303–308.

354 Belcastro AN, Arthur GD, Albisser TA, Raj DA (1996) Heart, liver, and skeletal muscle myeloperoxidase

355 activity during exercise. J Appl Physiol (1985) 80(4):1331–1335.

356 Boland B, Himpens B, Denef JF, Gillis JM (1995) Site-dependent pathological differences in smooth

357 muscles and skeletal muscles of the adult mdx mouse. Muscle Nerve 18(6):649–657.

358 Boldrin L, Zammit PS, Morgan JE (2015) Satellite cells from dystrophic muscle retain regenerative

359 capacity. Stem Cell Res 14(1):20–29. doi: 10.1016/j.scr.2014.10.007

360 Brickson S, Ji LL, Schell K, Olabisi R, St Pierre Schneider B, Best TM (2003) M1/70 attenuates

361 blood-borne neutrophil oxidants, activation, and myofiber damage following stretch injury. J Appl Physiol

362 (1985) 95(3):969–976.

363 Brussee V, Tardif F, Tremblay JP (1997) Muscle fibers of mdx mice are more vulnerable to exercise than

364 those of normal mice. Neuromuscul Disord 7(8):487–492.

365 Bulfield G, Siller WG, Wight PA, Moore KJ (1984) X chromosome-linked muscular dystrophy (mdx) in

366 the mouse. Proc Natl Acad Sci U S A 81(4):1189–1192.

367 Carpenter JL, Hoffman EP, Romanul FC, Kunkel LM, Rosales RK, Ma NS, Dasbach JJ, Rae JF, Moore

368 FM, McAfee MB, Pearce LK (1989) Feline muscular dystrophy with dystrophin deficiency. Am J Pathol

369 135(5):909–919.

370 Chargé SB, Rudnicki MA (2004) Cellular and molecular regulation of muscle regeneration. Physiol Rev

371 84(1):209–238.

372 Cheung EV, Tidball JG (2003) Administration of the non-steroidal anti-inflammatory drug ibuprofen

373 increases macrophage concentrations but reduces necrosis during modified muscle use. Inflamm Res

374 52(4):170–176.

375 Cooper BJ, Winand NJ, Stedman H, Valentine BA, Hoffman EP, Kunkel LM, Scott MO, Fischbeck KH,

376 Kornegay JN, Avery RJ, Williams JR, Schmickel RD, Sylvester JE (1988) The homologue of the

377 Duchenne locus is defective in X-linked muscular dystrophy of dogs. Nature 334(6178):154–156.

378 Coulton GR, Morgan JE, Partridge TA, Sloper JC (1988) The mdx mouse skeletal muscle myopathy: I. A

379 histological, morphometric and biochemical investigation. Neuropathol Appl Neurobiol 14(1):53–70.

380 Darr KC, Schultz E (1987) Exercise-induced satellite cell activation in growing and mature skeletal

381 muscle. J Appl Physiol (1985) 63(5):1816–1821.

382 De Luca A, Nico B, Liantonio A, Didonna MP, Fraysse B, Pierno S, Burdi R, Mangieri D, Rolland JF,

383 Camerino C, Zallone A, Confalonieri P, Andreetta F, Arnoldi E, Courdier-Fruh I, Magyar JP, Frigeri A,

384 Pisoni M, Svelto M, Conte Camerino D (2005) A multidisciplinary evaluation of the effectiveness of

385 cyclosporine a in dystrophic mdx mice. Am J Pathol 166(2):477–489.

386 Emery AE (1989) Clinical and molecular studies in Duchenne muscular dystrophy. Prog Clin Biol

387 306:15–28.

388 Farini A, Meregalli M, Belicchi M, Battistelli M, Parolini D, D'Antona G, Gavina M, Ottoboni L,

389 Constantin G, Bottinelli R, Torrente Y (2007) T and B lymphocyte depletion has a marked effect on the

390 fibrosis of dystrophic skeletal muscles in the scid/mdx mouse. J Pathol 213(2):229–238.

391 Fielding RA, Manfredi TJ, Ding W, Fiatarone MA, Evans WJ, Cannon JG (1993) Acute phase response in

392 exercise. III. Neutrophil and IL-1 beta accumulation in skeletal muscle. Am J Physiol 265(1 Pt 2):R166 –

393 R172.

394 Gehrig SM, Koopman R, Naim T, Tjoakarfa C, Lynch GS (2010) Making fast-twitch dystrophic muscles

395 bigger protects them from contraction injury and attenuates the dystrophic pathology. Am J Pathol

396 176(1):29–33. doi: 10.2353/ajpath.2010.090760

397 Granchelli JA, Pollina C, Hudecki MS (2000) Pre-clinical screening of drugs using the mdx mouse.

398 Neuromuscul Disord 10(4-5):235–239.

399 Grounds MD (1987) Phagocytosis of necrotic muscle in muscle isografts is influenced by the strain, age,

400 and sex of host mice. J Pathol 153(1):71–82.

401   Grounds MD, Torrisi J (2004) Anti-TNFalpha (Remicade) therapy protects dystrophic skeletal muscle

402   from necrosis. FASEB J 18(6):676–682.

403   Heydemann A, Swaggart KA, Kim GH, Holley-Cuthrell J, Hadhazy M, McNally EM (2012) The

404   superhealing MRL background improves muscular dystrophy. Skelet Muscle 2(1):26. doi:

405   10.1186/2044-5040-2-26

406   Hindi SM, Shin J, Ogura Y, Li H, Kumar A (2013) Matrix metalloproteinase-9 inhibition improves

407   proliferation and engraftment of myogenic cells in dystrophic muscle of mdx mice. PLoS One

408   8(8):e72121. doi: 10.1371/journal.pone.0072121

409   Hodgetts S, Radley H, Davies M, Grounds MD (2006) Reduced necrosis of dystrophic muscle by

410   depletion of host neutrophils, or blocking TNFalpha function with Etanercept in mdx mice. Neuromuscul

411   Disord 16(9-10):591–602.

412   Le Grand F, Rudnicki M (2007) Satellite and stem cells in muscle growth and repair. Development

413   134(22):3953–3957.

414   Lescaudron L, Peltékian E, Fontaine-Pérus J, Paulin D, Zampieri M, Garcia L, Parrish E (1999) Blood

415   borne macrophages are essential for the triggering of muscle regeneration following muscle transplant.

416   Neuromuscul Disord 9(2):72–80.

417   Li H, Mittal A, Makonchuk DY, Bhatnagar S, Kumar A (2009) Matrix metalloproteinase-9 inhibition

418   ameliorates pathogenesis and improves skeletal muscle regeneration in muscular dystrophy. Hum Mol

419   Genet 18(14):2584–2598. doi: 10.1093/hmg/ddp191

420   Lockhart NC, Brooks SV (2008) Neutrophil accumulation following passive stretches contributes to

421   adaptations that reduce contraction-induced skeletal muscle injury in mice. J Appl Physiol (1985)

422   104(4):1109–1115. doi: 10.1152/japplphysiol.00850.2007

423   Louboutin JP, Fichter-Gagnepain V, Thaon E, Fardeau M (1993) Morphometric analysis of mdx

424   diaphragm muscle fibers. Comparison with hindlimb muscles. Neuromuscul Disord 3(5-6):463–469.

425   McGeachie JK, Grounds MD, Partridge TA, Morgan JE (1993) Age-related changes in replication of

426 myogenic cells in mdx mice: quantitative autoradiographic studies. J Neurol Sci 119(2):169–179.

427 McLoughlin TJ, Tsivitse SK, Edwards JA, Aiken BA, Pizza FX (2003) Deferoxamine reduces and nitric

428 oxide synthase inhibition increases neutrophil-mediated myotube injury. Cell Tissue Res 313(3):313–319.

429 Merly F, Lescaudron L, Rouaud T, Crossin F, Gardahaut MF (1999) Macrophages enhance muscle

430 satellite cell proliferation and delay their differentiation. Muscle Nerve 22(6):724–732.

431 Morrison J, Lu QL, Pastoret C, Partridge T, Bou-Gharios G (2000) T-cell-dependent fibrosis in the mdx

432 dystrophic mouse. Lab Invest 80(6):881–891.

433 Mojumdar K, Liang F, Giordano C, Lemaire C, Danialou G, Okazaki T, Bourdon J, Rafei M, Galipeau J,

434 Divangahi M, Petrof BJ (2014) Inflammatory monocytes promote progression of Duchenne muscular

435 dystrophy and can be therapeutically targeted via CCR2. EMBO Mol Med 6(11):1476-1492.

436 Nguyen HX, Tidball JG (2003) Expression of a muscle-specific, nitric oxide synthase transgene prevents

437 muscle membrane injury and reduces muscle inflammation during modified muscle use in mice. J Physiol

438 550(Pt 2):347–356.

439 Nguyen HX, Tidball JG (2003) Interactions between neutrophils and macrophages promote macrophage

440 killing of rat muscle cells in vitro. J Physiol 547(Pt 1):125–132.

441 Orimo S, Hiyamuta E, Arahata K, Sugita H (1991) Analysis of inflammatory cells and complement C3 in

442 bupivacaine-induced myonecrosis. Muscle Nerve 14(6):515–520.

443 Pastoret C, Sebille A (1995) Mdx mice show progressive weakness and muscle deterioration with age. J

444 Neurol Sci 129(2):97–105.

445 Pierezan F, Mansell J, Ambrus A, Rodrigues Hoffmann A (2014) Immunohistochemical expression of

446 ionized calcium binding adapter molecule 1 in cutaneous histiocytic proliferative, neoplastic and

447 inflammatory disorders of dogs and cats. J Comp Pathol 151:347-351.

448 Pizza FX, Koh TJ, McGregor SJ, Brooks SV (2001) Muscle inflammatory cells after passive stretches,

449 isometric contractions and lengthening contractions. J Appl Physiol (1985) 92(5):1873–1878.

450 Pizza FX, McLoughlin TJ, McGregor SJ, Calomeni EP, Gunning WT (2001) Neutrophils injure cultured

451   skeletal myotubes. Am J Physiol Cell Physiol 281(1):C335–C341.

452   Pizza FX, Peterson JM, Baas JH, Koh TJ (2005) Neutrophils contribute to muscle injury and impair its

453   resolution after lengthening contractions in mice. J Physiol 562(Pt 3):899–913.

454   Porter JD, Khanna S, Kaminski HJ, Rao JS, Merriam AP, Richmonds CR, Leahy P, Li J, Guo W, Andrade

455   FH (2002) A chronic inflammatory response dominates the skeletal muscle molecular signature in

456   dystrophin-deficient mdx mice. Hum Mol Genet 11(3):263–272.

457   Porter JD, Merriam AP, Leahy P, Gong B, Feuerman J, Cheng G, Khanna S (2004) Temporal gene

458   expression profiling of dystrophin-deficient (mdx) mouse diaphragm identifies conserved and muscle

459   group-specific mechanisms in the pathogenesis of muscular dystrophy. Hum Mol Genet 13(3):257–269.

460   Robertson TA, Maley MA, Grounds MD, Papadimitriou JM (1993) The role of macrophages in skeletal

461   muscle regeneration with particular reference to chemotaxis. Exp Cell Res 207(2):321–331.

462   Schneider JS, Shanmugam M, Gonzalez JP, Lopez H, Gordan R, Fraidenraich D, Babu GJ (2013)

463   Increased sarcolipin expression and decreased sarco(endo)plasmic reticulum Ca2+ uptake in skeletal

464   muscles of mouse models of Duchenne muscular dystrophy. J Muscle Res Cell Motil 34(5-6):349-356.

465   doi: 10.1007/s10974-013-9350-0

466   Shavlakadze T, White J, Hoh JF, Rosenthal N, Grounds MD (2004) Targeted expression of insulin-like

467   growth factor-I reduces early myofiber necrosis in dystrophic mdx mice. Mol Ther 10(5):829–843.

468   Snow MH (1977) Myogenic cell formation in regenerating rat skeletal muscle injured by mincing. II. An

469   autoradiographic study. Anat Rec 188(2):201–217.

470   Snow MH (1978) An autoradiographic study of satellite cell differentiation into regenerating myotubes

471   following transplantation of muscles in young rats. Cell Tissue Res 186(3):535–540.

472   Stedman HH, Sweeney HL, Shrager JB, Maguire HC, Panettieri RA, Petrof B, Narusawa M, Leferovich

473   JM, Sladky JT, Kelly AM (1991). The mdx mouse diaphragm reproduces the degenerative changes of

474   Duchenne muscular dystrophy. Nature 352(6335):536–539.

475   Tedesco FS, Dellavalle A, Diaz-Manera J, Messina G, Cossu G (2010) Repairing skeletal muscle:

476   regenerative potential of skeletal muscle stem cells. J Clin Invest 120(1):11–19. doi: 10.1172/JCI40373

477   Ten Broek RW, Grefte S, Von den Hoff JW (2010) Regulatory factors and cell populations involved in

478   skeletal muscle regeneration. J Cell Physiol 224(1):7–16. doi: 10.1002/jcp.22127

479   Tidball JG (2005) Inflammatory processes in muscle injury and repair. Am J Physiol Regul Integr Comp

480   Physiol 288(2):R345–R353.

481   Tsivitse S (2010) Notch and Wnt signaling, physiological stimuli and postnatal myogenesis. Int J Biol Sci

482   6(3):268–281.

483   Walden DL, McCutchan HJ, Enquist EG, Schwappach JR, Shanley PF, Reiss OK, Terada LS, Leff JA,

484   Repine JE (1990) Neutrophils accumulate and contribute to skeletal muscle dysfunction after

485   ischemia-reperfusion. Am J Physiol 259(6 Pt 2):H1809–H1812.

486   Weller B, Karpati G, Carpenter S (1990) Dystrophin-deficient mdx muscle fibers are preferentially

487   vulnerable to necrosis induced by experimental lengthening contractions. J Neurol Sci 100(1-2):9–13.

488   Zacks SI, Sheff MF (1982) Age-related impeded regeneration of mouse minced anterior tibial muscle.

489   Muscle Nerve 5(2):152–161.

490

491   **Figure Legends**

492   **Fig. 1** Age-dependent changes in phenotypes of B10 and mdx mice.

493   (**A**) Comparison of body weights between B10 and mdx mice. Values = mean ± SE. B10: n ≥ 4; mdx: n

494   ≥ 10. *: $P < 0.01$ vs B10 at same age, Mann-Whitney U-test.

495   (**B**) Transverse sections of triceps brachii muscle from B10 and mdx mice stained with Masson's

496   trichrome stain at 4 and 6 weeks of age. Bars = 1 mm (low magnification), 100 μm (high magnification).

497

498   **Fig. 2** Comparison of myofibers between B10 (left) and mdx mice (right).

499   Transverse sections of triceps brachii muscle (TB) and costal part of the diaphragm (CPD) stained with

500   Masson's trichrome stain at 6 weeks of age. Squared areas within low magnification images are

501 magnified in the right panels. B10 mice show no histopathological change in either TB or CPD. In mdx

502 mice, degenerative myofibers (arrows, magnified panel of TB) are characterized by faint-colored and

503 disrupting myofibers. Regenerating myofibers (small arrowheads, magnified panel of TB) are small and

504 basophilic myofibers with central nuclei. Regenerated myofibers (large arrowheads, magnified panel of

505 TB and CPD) have eosinophilic large myofibers and non-peripheral (including central) nuclei in mdx

506 mice. Bars = 100 μm (low magnification), 20 μm (high magnification). w: weeks of age.

507

508 **Fig. 3** Regenerative features of skeletal muscle lesions in mdx mice.

509 Transverse sections of the same area of triceps brachii muscle in mdx mice at 4 weeks of age.

510 Hematoxylin and eosin staining (**A, D, G, and J**) and immunohistochemical staining for embryonic

511 myosin heavy chain (eMyHC) (B, E, H, and K) and paired box 7 (PAX7) (**C, F, I, and L**). Numerous

512 PAX7-positive muscle satellite cells surround eMyHC-positive regenerating myofibers in skeletal

513 muscles of mdx mice (**A–F**), and the number of the former and the staining intensity of the latter

514 gradually decrease with progression of myofiber regeneration (**A–C and G–L**). Bars = 100 μm (low

515 magnification), 20 μm (high magnification).

516

517 **Fig. 4** Ratio of degenerative and regenerative myofibers in skeletal muscles in mdx mice.

518 Myofibers classified into normal myofibers (**A**), degenerative myofibers (**B**), centronucleated myofibers

519 (**C**), regenerating myofibers (**D**), or regenerated myofibers (**E**). The sum of values of regenerating

520 myofibers and regenerated myofibers indicates the values of centronucleated myofibers. CT, cranial tibial

521 muscle; GA, gastrocnemius muscle; QR, quadriceps femoris muscle; TB, triceps brachii muscle; LL,

522 lumbar longissimus muscle; CPD, costal part of the diaphragm. Statistically significant differences among

523 muscles from mice of the same age are indicated by different letters (C, G, Q, T, and D indicating CT, GA,

524 QR, TB and CPD, respectively). Significant age differences between samples of the same muscle are

525 indicated by symbols (* and†). Analyses were performed using Kruskal-Wallis test, followed by Scheffé's

526   method for multiple comparisons when a significant difference is observed ($P < 0.05$). Values = mean ±

527   SE; 4 w, n = 4; 6 w and 14 w, n = 3. w: weeks of age

528

529   **Fig. 5** Infiltration of immune cells in skeletal muscle lesions in mdx mice.

530   (**A–D**) Immunohistochemical staining for Iba1, Gr1, B220, and CD3 in triceps brachii muscle of mdx

531   mice at 6 weeks of age. Bars: 100 μm (panels), 20 μm (insets).

532   (**E–H**) Comparison of the number of inflammatory cells in each skeletal muscle for mice at different ages.

533   See Figure 4 legend for abbreviations. Statistically significant differences among muscles from mice of

534   the same age are indicated by different letters (C, G, Q, T, and D indicating CT, GA, QR, TB, and CPD,

535   respectively). Significant age differences between samples of the same muscle are indicated by symbols

536   (* and†). Analyses were performed using Kruskal-Wallis test, followed by Scheffé's method for multiple

537   comparisons when a significant difference was observed ($P < 0.05$). Values = mean ± SE. 4 w, n = 4; 6 w

538   and 14 w, n = 3. w: weeks of age

539

540   **Fig. 6** Correlation between inflammatory cell infiltration and ratio of degenerating, regenerating, and

541   regenerated myofibers in mdx mice.

542   Graph showing Spearman's rank correlations between the density of inflammatory cells (Iba1: a-c, Gr1:

543   d-f, B220: g-i, and CD3: j-l) and the ratio of degenerating (a, d, g and j), regenerating (b, e, h and k), and

544   regenerated (c, f, i and l) myofibers.*: $P < 0.05$, Spearman's rank correlation test; ρ: Spearman's rank

545   correlation coefficient. n = 29.

546

547　**Table 1** Antibodies, working dilutions, and methods for antigen retrieval

Antibody	Source	Dilution	Antigen retrieval	Heating condition
Mouse anti-eMyHC	DSHB (Iowa, USA)	1:900	20 mM Tris-HCl (pH 9.0)	105°C, 20 minutes
Mouse anti-PAX7	DSHB (Iowa, USA)	1:200	20 mM Tris-HCl (pH 9.0)	105°C, 20 minutes
Rabbit anti-Iba1	Wako (Osaka, Japan)	1:2000	0.1% pepsin/ 0.2 N HCl	37°C, 5 minutes
Rat anti-Gr1	R and D system (Minneapolis, USA)	1:800	0.1% pepsin/ 0.2 N HCl	37°C, 5 minutes
Rat anti-B220	Cedarlane (Ontario, Canada)	1:1600	20 mM Tris-HCl (pH 9.0)	105°C, 20 minutes
Rabbit anti-CD3	Nichirei (Tokyo, Japan)	1:500	20 mM Tris-HCl (pH 9.0)	105°C, 20 minutes

Fig. 1 Age-dependent changes in phenotypes of B10 and mdx mice.
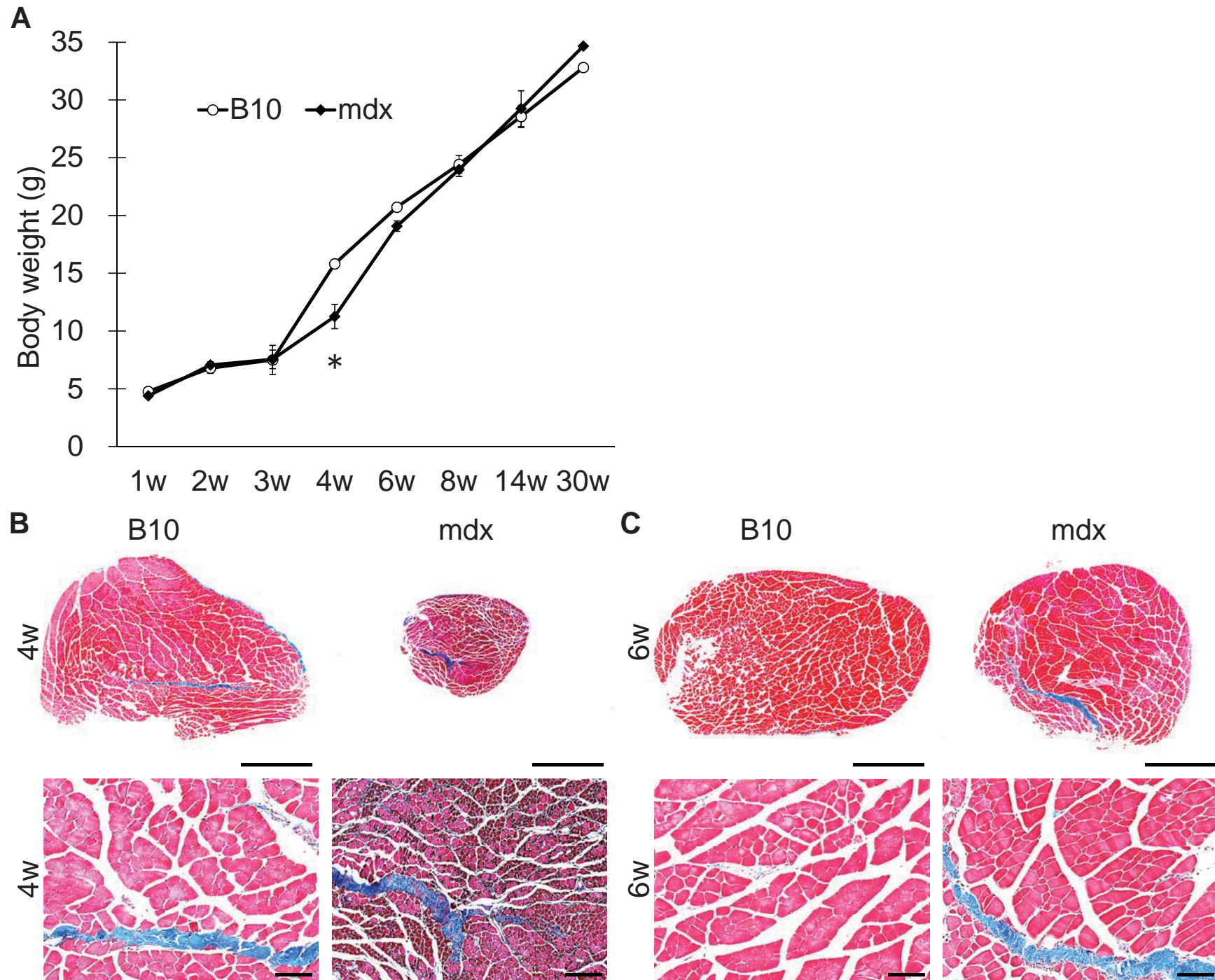
Fig. 2 Comparison of myofibers between B10 (left) and mdx mice (right).
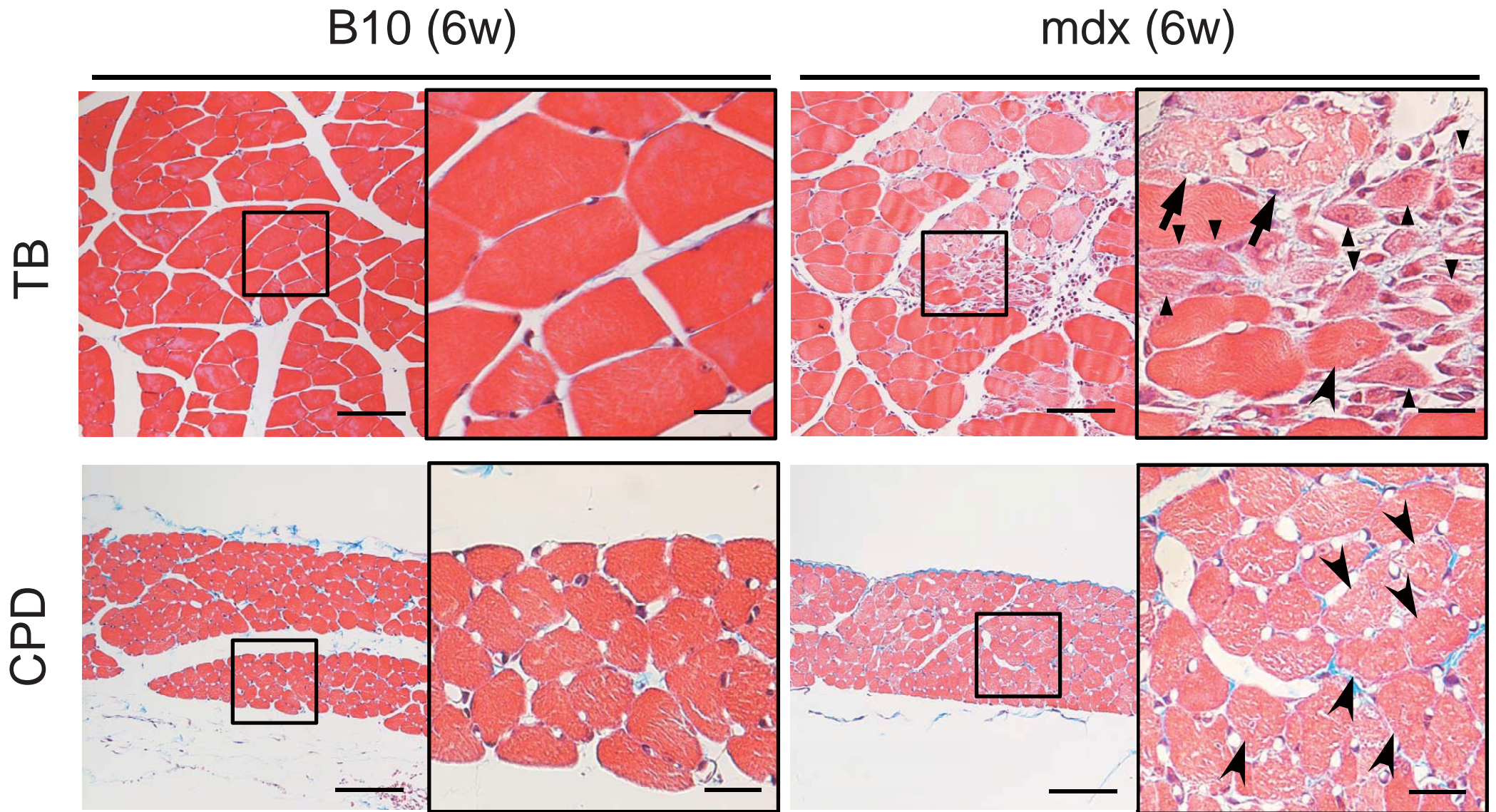
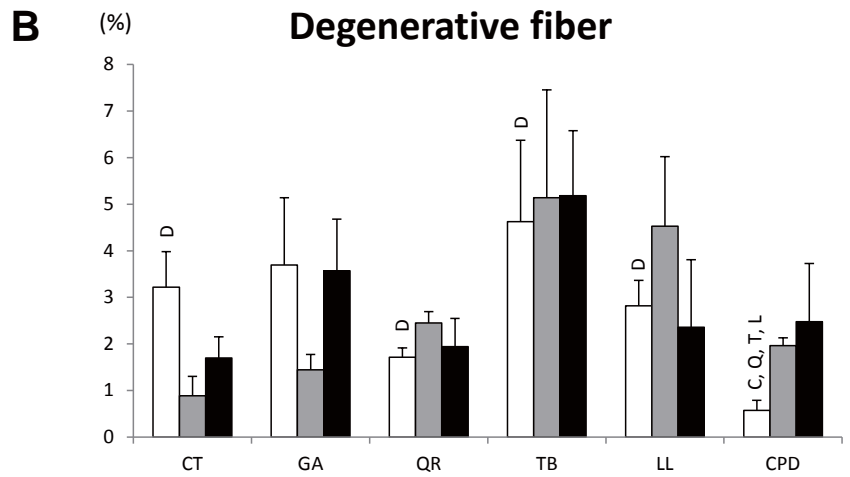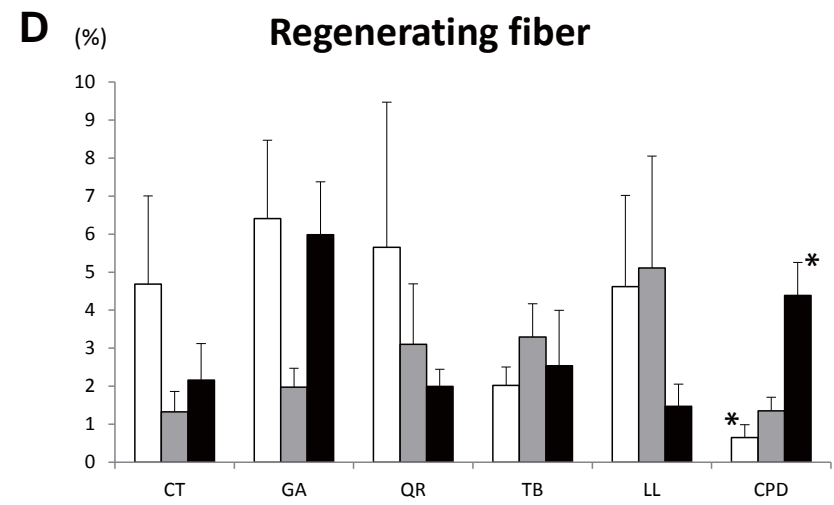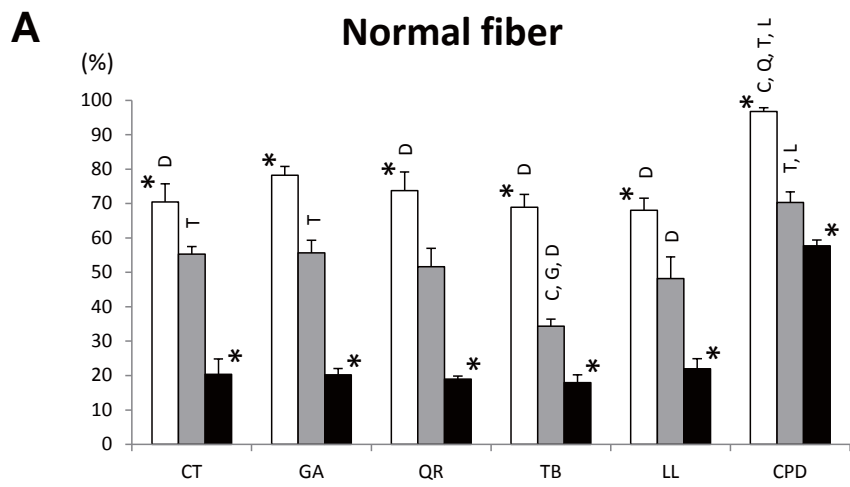**Fig. 3 Regenerative features of skeletal muscle lesions in mdx mice.**
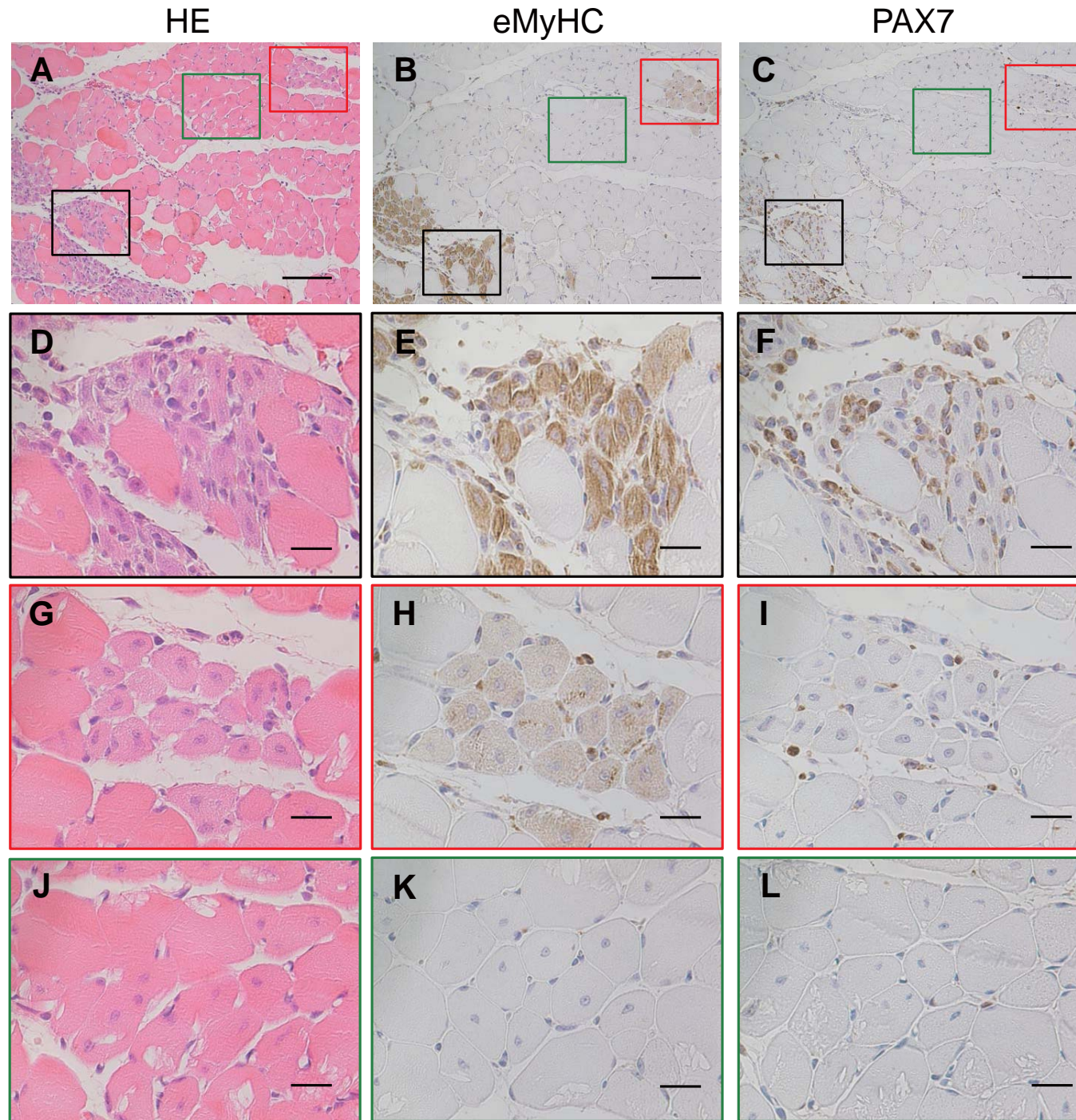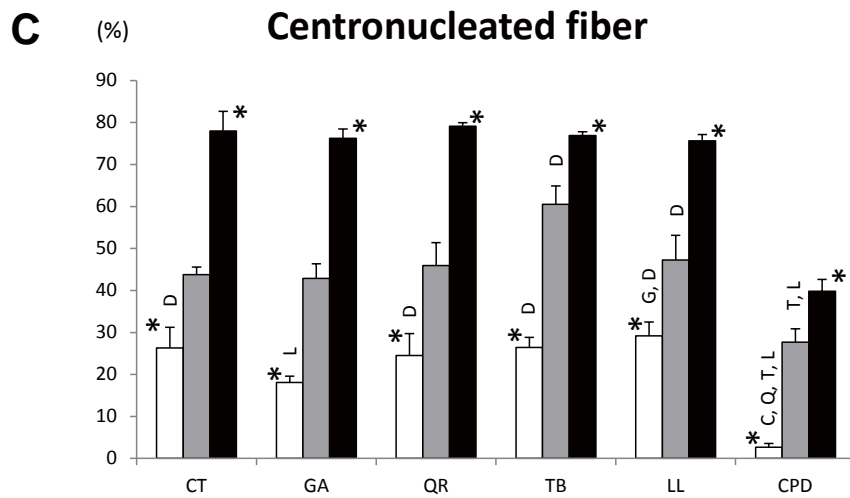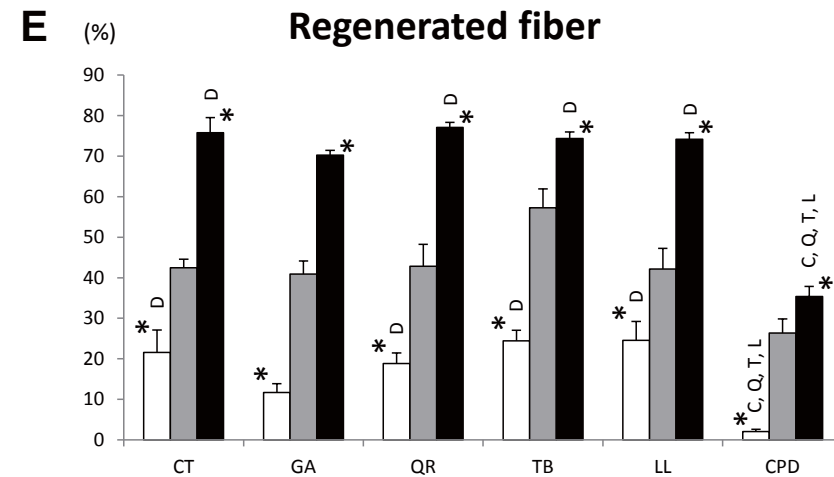
Fig. 4 Ratio of degenerative and regenerative myofibers in skeletal muscles in mdx mice.

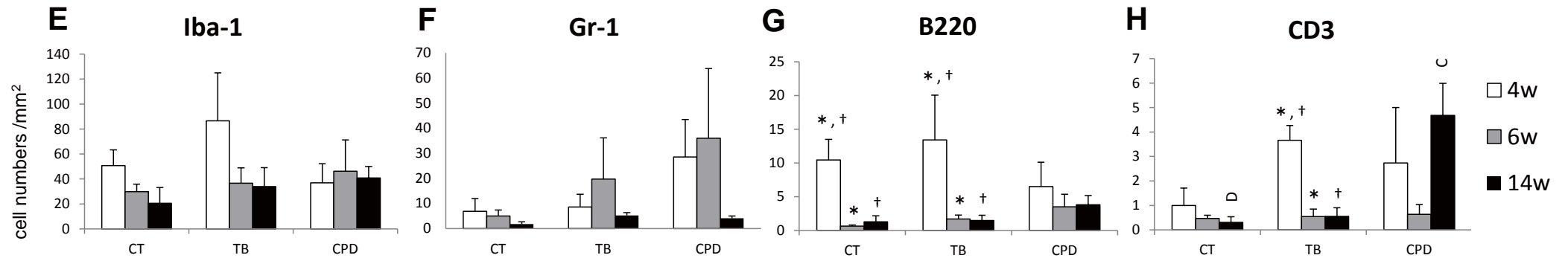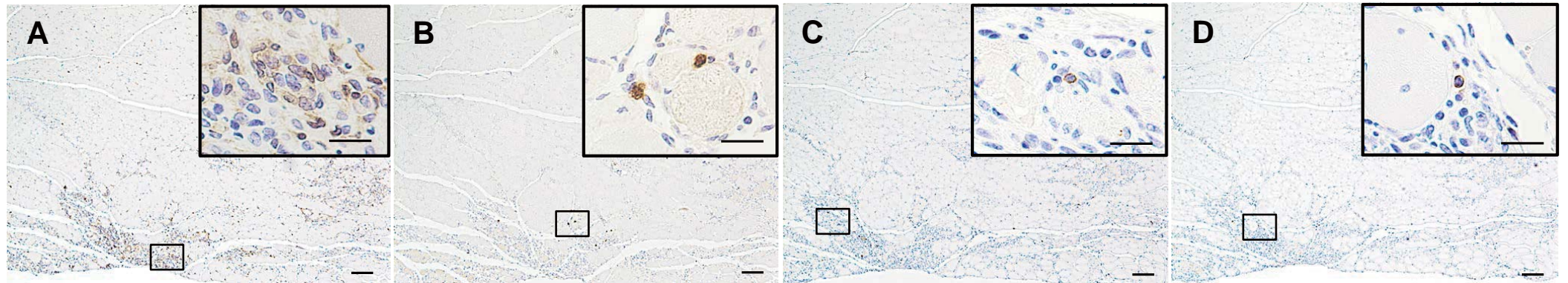**Fig. 5 Infiltration of immune cells in skeletal muscle lesions in mdx mice.**

Fig. 6 Correlation between inflammatory cell infiltration and ratio of degenerating, regenerating, and regenerated myofibers in mdx mice.